

Tuning bimolecular chemical reactions by electric fields

Timur V. Tscherbul^{1,2} and Roman V. Krems²

¹*Chemical Physics Theory Group, Department of Chemistry,
and Center for Quantum Information and Quantum Control,
University of Toronto, Toronto, Ontario, M5S 3H6, Canada*

²*Department of Chemistry, University of British Columbia,
Vancouver, British Columbia, V6T 1Z1, Canada*

(Dated: September 23, 2014)

We develop a theoretical method for solving the quantum mechanical reactive scattering problem in the presence of external fields based on a hyperspherical coordinate description of the reaction complex combined with the total angular momentum representation for collisions in external fields. The method allows us to obtain converged results for the chemical reaction $\text{LiF} + \text{H} \rightarrow \text{Li} + \text{HF}$ in an electric field. Our calculations demonstrate that, by inducing couplings between states of different total angular momenta, electric fields with magnitudes < 150 kV/cm give rise to resonant scattering and a significant modification of the total reaction probabilities, product state distributions and the branching ratios for reactive vs inelastic scattering.

Tuning microscopic chemical reactions with external fields has long been an ultimate goal in chemical reaction dynamics [1]. This goal stimulated the development of quantum control schemes [2, 3], which have been applied with spectacular results to unimolecular reactions. Attaining control over bimolecular reactions in a gas has proven to be a much bigger challenge due to the randomness of the rotational and translational motion of the reactants [4, 5]. This randomness can be reduced by cooling molecules to low temperatures [4, 6]. Recent experiments [7–9] demonstrated that chemical reactions in an ultracold gas of KRb molecules can be effectively suppressed by applying an electric field. While demonstrating that the randomness of the molecular motion can be harnessed, the control mechanism in Refs. [7, 8] amounts to switching off reactive collisions by tunable long-range barriers, which prevent the reactants from approaching close enough to undergo chemical transformations.

In general, for chemical reactions to occur, molecules must approach each other at close range, where the interactions induced by external fields (typically ~ 1 K in magnitude) must compete with strong intermolecular interactions (often > 1000 K) at short separations between the reactants. Since the external field-induced couplings are so small compared to intermolecular interactions, it is not clear if external fields can be used to steer chemical reactions. For example, the effects of external fields on the product state distributions and branching ratios for different reaction channels remain completely unknown. It is expected that the rates of low-temperature chemical reactions must be significantly affected by scattering resonances [5]. However, it is not known if scattering resonances capable of affecting the outcome of a chemical reaction can be induced by electric or magnetic fields with feasible strengths.

These questions stimulated the mounting number of experiments [10] and several quantum threshold models [11] and quantum defect theories [12, 13] were proposed to describe the observations. While these models provide

valuable insight into the effect of long-range interactions on ultracold reactions, they do not describe the reaction dynamics at short range and thus can be applied to model only the averaged quantities such as the total reaction rates. The detailed dynamics of chemical reactions is most accurately encoded in the state-to-state scattering S -matrices, which can be obtained by quantum reactive scattering calculations. However, even in the absence of external fields, the quantum reactive scattering problem is challenging due to the presence of multiple reaction arrangements (the coordinate problem) and the computational expense due to a large number of rovibrational states involved in a chemical reaction [14–17]. The presence of external fields further complicates the problem, making it necessary to consider the coupling between states with different total angular momenta of the reaction complex.

In this Letter, we report the first numerically exact quantum scattering calculation on a chemical reaction in an external field. Using a newly developed theoretical approach based on hyperspherical coordinates [14, 16] combined with the total angular momentum representation for collisions in external fields [18, 19], we show that the total cross section and the nascent product state distribution of an atom-diatom reaction ($\text{LiF} + \text{H} \rightarrow \text{Li} + \text{HF}$) at low collision energies can be effectively controlled by DC electric fields with affordable strengths. Our results show that electric fields can have a dramatic effect on chemical reactivity at low temperatures by inducing tunable reactive scattering resonances.

We begin by outlining our quantum reactive scattering approach. For a three-atom reaction, there are three reaction arrangements, $\text{Li} + \text{HF}$, $\text{H} + \text{LiF}$ and $\text{F} + \text{LiH}$, that need to be considered simultaneously. To do this, we use the Fock-Delves (FD) hyperspherical coordinates. Expressed in these coordinates, the Hamiltonian of the atom-molecule reaction complex in the presence of an

external field is [14, 16, 17]

$$\hat{H} = \frac{-1}{2\mu\rho^5} \frac{\partial}{\partial\rho} \rho^5 \frac{\partial}{\partial\rho} + \frac{(\hat{\mathbf{J}} - \hat{\mathbf{j}}_\alpha)^2}{2\mu\rho^2 \cos^2 \theta_\alpha} + V(\rho, \theta_\alpha, \gamma_\alpha) + \hat{H}_{\text{mol},\alpha} \quad (1)$$

where $\rho = (R_\alpha^2 + r_\alpha^2)^{1/2}$ is the hyperradius, θ_α and γ_α are the hyperangles defined by $\tan \theta_\alpha = r_\alpha/R_\alpha$, and $\cos \gamma_\alpha = (\mathbf{R}_\alpha \cdot \mathbf{r}_\alpha)/(R_\alpha r_\alpha)$, and \mathbf{R}_α and \mathbf{r}_α are mass-scaled Jacobi vectors in arrangement $\alpha = 1, 2, 3$ [14].

In Eq. (1), $\hat{\mathbf{J}}$ is the total angular momentum of the reaction complex and $\hat{\mathbf{j}}_\alpha$ is the rotational angular momentum of the diatomic molecule in arrangement α . The interaction of the reactants and products with the external field is included in the last term of Eq. (1). For reactions in a DC electric field, this term is [17]

$$\hat{H}_{\text{mol},\alpha} = \frac{-1}{2\mu\rho^2 \sin^2 2\theta_\alpha} \frac{\partial}{\partial\theta_\alpha} \sin^2 2\theta_\alpha \frac{\partial}{\partial\theta_\alpha} + \frac{\hat{\mathbf{j}}_\alpha^2}{2\mu\rho^2 \sin^2 \theta_\alpha} + V_\alpha(\rho, \theta_\alpha) - \mathbf{d}_\alpha(\rho, \theta_\alpha) \cdot \mathbf{E}, \quad (2)$$

where \mathbf{d}_α is the electric dipole moment of the diatomic molecule in arrangement α and \mathbf{E} is the electric field vector, which defines a space-fixed (SF) quantization axis. The wavefunction of the reaction complex is expanded in hyperspherical adiabatic surface functions

$$\Psi = \rho^{-5/2} \sum_i F_i(\rho) \Phi_i(\rho; \Omega), \quad (3)$$

where $\Phi_i(\Omega)$ are obtained by solving the adiabatic eigenvalue problem $\hat{H}_{\text{ad}} \Phi_i(\Omega; \rho) = \epsilon_i(\rho) \Phi_i(\Omega; \rho)$, $\epsilon_i(\rho)$ are the adiabatic hyperspherical energies, and \hat{H}_{ad} is the adiabatic surface Hamiltonian obtained by subtracting the hyperradial kinetic energy from the full Hamiltonian in Eq. (1) [14, 16, 17]. To solve the eigenvalue problem, we expand the surface functions as [16, 18, 19]

$$\Phi_i(\rho; \Omega) = \sum_{\alpha, v, j, J, k, \eta} W_{\alpha v j J k \eta, i} |\alpha v j J k \eta\rangle \quad (4)$$

where $|\alpha v j J k \eta\rangle = |JMk\rangle 2\chi_{\alpha v j}(\theta_\alpha; \rho)/(\sin 2\theta_\alpha)$ and $\chi_{\alpha v j}(\theta_\alpha; \rho)$ are the primitive FD basis functions, which diagonalize the Hamiltonian in Eq. (2) at *zero field* [17]. The states $|JMk\rangle$ are the symmetry-adapted angular basis functions,

$$|JMk\rangle = N_k [|JMk\rangle |jk\rangle + \eta(-1)^J |JM-k\rangle |j-k\rangle], \quad (5)$$

composed of the spherical harmonics $|jk\rangle = \sqrt{2\pi} Y_{jk}(\theta_\alpha, 0)$ and the symmetric top eigenfunctions $|JMk\rangle$, where η is the inversion parity, M and k are the projections of J on the SF and body-fixed quantization axes, respectively [14], and $N_k = [2(1 + \delta_{k0})]^{-1/2}$. The basis (4) is key to the efficiency of the method we propose here. In an external field, J and η are not conserved but the matrix of the field-induced interaction in the basis (4) is tridiagonal in J and thus only a

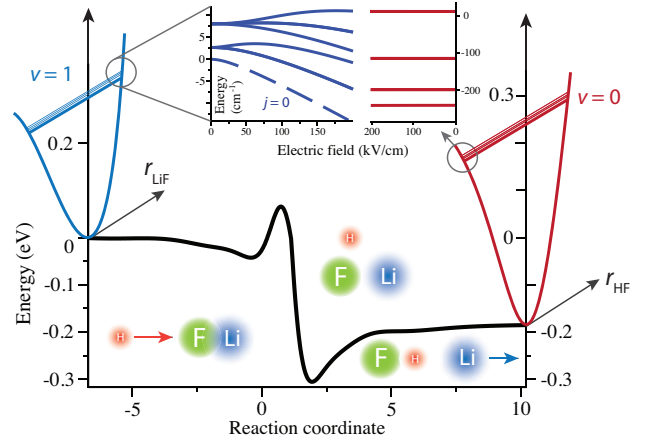


Fig. 1: (Upper panel) Schematic diagram of the $\text{LiF} + \text{H} \rightarrow \text{HF} + \text{Li}$ chemical reaction showing (1) the minimum energy path along the reaction coordinate $s = r_{\text{LiF}} - r_{\text{HF}}$ (2) vibrational potential energy curves of the reactants and products and (3) the Stark structure of the LiF and HF molecules in the entrance reaction channel (not to scale).

limited number of J -states is generally required for a fully converged calculation [19]. This offers a great computational advantage over the previously proposed approach to reactive scattering in external fields [17], which disregards the total angular momentum of the reaction complex. All calculations are performed using the quantum reactive scattering program ABC [15], extensively modified to incorporate the effects of electric fields (see the Supplementary Material [20]).

We now apply the newly developed methodology to study the effects of electric fields on the chemical reaction $\text{LiF} + \text{H} \rightarrow \text{HF} + \text{Li}$. The choice of the reaction is motivated by the large permanent electric dipole moment of LiF ($d = 6.3$ D), thus leading one to expect large electric field effects in the entrance reaction channel, but not in the outgoing channels [17]. In addition, the inverse reaction $\text{Li} + \text{HF} \rightarrow \text{LiF} + \text{H}$ has been the focus of numerous theoretical and experimental studies [21–24]. An experimental study of its low-temperature dynamics is in progress using a rotating nozzle source of HF molecules combined with a magneto-optical trap for Li atoms [24]. The reaction $\text{LiF} + \text{H} \rightarrow \text{LiF} + \text{H}$ can similarly be studied using a cold ensemble of H atoms confined in a magnetic trap [25, 26] combined with a slow beam of LiF molecules [27, 28].

To describe the atom-molecule interaction $V(\rho, \theta_\alpha, \gamma_\alpha)$ in the LiHF reaction complex, we use an accurate *ab initio* potential energy surface (PES) [22] previously employed in field-free reaction rate calculations at low temperatures [23]. Figure 1 illustrates the key features of the PES. The reaction proceeds through a transition state that has a bent configuration and the barrier height is 518 cm^{-1} relative to the bottom of the LiF potential well [22]. The chemical reaction $\text{LiF}(v=1, j=0) + \text{H} \rightarrow$

$\text{HF}(v=0, j=0) + \text{Li}$ is slightly exoergic ($\Delta E = 0.1$ eV), and a total of 6 HF rotational states are energetically accessible at zero collision energy.

Figure 2 shows the total cross section for HF production in the chemical reaction of $\text{LiF}(v=1, j=0)$ with H as a function of the electric field strength. At low temperatures, the reaction occurs by the tunneling of a heavy F atom [23] and hence the reaction cross section is small. An applied electric field accelerates the chemical reaction. We attribute this effect to the field-induced orientation of LiF, leading to hybridization of the ground rotational state $j=0$ with higher-energy rotational states $j>0$, which helps the reactants to effectively surmount the potential barrier. This increase of the chemical reactivity must be sensitive to the tunneling probability under the reaction barrier at the bottom of the barrier so the electric field dependence of the reaction cross sections can be used as a probe of the reaction barrier width.

The most remarkable feature apparent in Fig. 2 is a pronounced resonance triplet at $E \sim 125$ kV/cm (peaks A, B, and C). The central resonance B corresponds to an electric-field-induced enhancement of chemical reactivity by a factor of 42. Resonances A and B have the same width of ~ 0.4 kV/cm, while resonance B is 10 times narrower. The following analysis suggests that the enhancement is due to a *field-induced* resonance in the *outgoing* reaction channel. This exquisite kind of scattering resonance is specific to low-energy dynamics of systems with anisotropic interactions (such as magnetic atoms [29, 30], atom-molecule mixtures [31], and polar molecules [32]). The search for reactive scattering resonances and their effects on dynamical observables has been a major thrust in chemical reaction dynamics for several decades [21, 33, 34]. Unlike the Feshbach or shape resonances explored before at higher collision energies [33, 34], the low-energy reactive scattering resonances shown in Fig. 2 can be tuned by an electric field.

We next consider another important observable property of a chemical reaction, the nascent product state distribution $\sigma_{\alpha v j \rightarrow \alpha' v' j'} / \sum_{\alpha' v' j'} \sigma_{\alpha v j \rightarrow \alpha' v' j'}$, where $\sigma_{\alpha v j \rightarrow \alpha' v' j'}$ is the cross section for the $\alpha v j \rightarrow \alpha' v' j'$ reaction process. This distribution quantifies the amount of internal energy with which the reaction products form. Fig. 2 shows that low-to-moderate electric fields modify the rotational distributions of HF by changing the relative populations of $j'=3$ and $j'=5$. As shown below, this effect occurs due to the emergence of new chemical reaction pathways forbidden at zero fields by total angular momentum conservation.

At $E \sim 125 - 127$ kV/cm corresponding to the field-induced resonances A, B, and C, the shape of the nascent product state distribution changes dramatically. Away from the resonances, we observe a “hot” HF product distribution that peaks at $j'=5$ and falls off gradually with decreasing j' . This pattern is characteristic of a quasi-resonant reaction mechanism [35], which favors population of rotational levels with smallest energy gaps

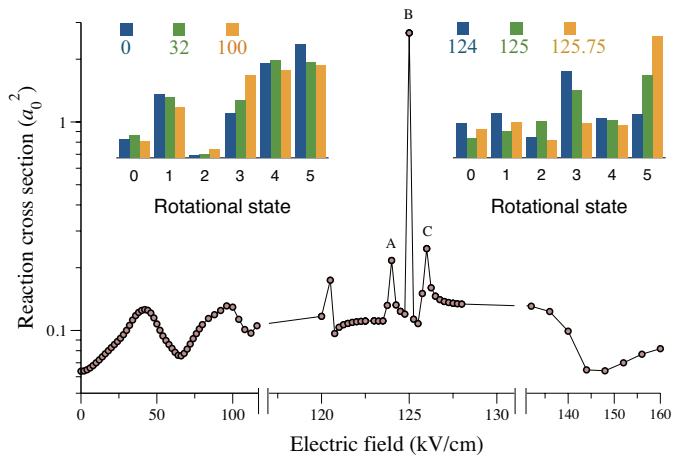


Fig. 2: Electric field dependence of the total cross section for the reaction $\text{LiF} + \text{H} \rightarrow \text{HF} + \text{Li}$. The insets show the nascent rotational state distributions of HF molecules produced in the reaction as a function of the final rotational state j' at electric field strengths of 0, 32 and 100 kV/cm (left) and 124, 125 and 125.75 kV/cm (right). Note the dramatic change in the shape of the distribution near the resonance electric field (right inset). The collision energy $E_C = 0.01$ cm^{-1} .

between the incoming and outgoing reaction channels. On resonance A, the distribution develops a pronounced peak at $j'=3$ and behaves non-monotonically as a function of j' , indicating a dramatic change in the reaction mechanism across a narrow interval of electric fields. On resonance B, the HF products are formed with a more even distribution over rotational energy levels, with $j'=2-5$ all substantially populated. As the electric field is tuned across resonance C, a unimodal distribution develops centered at $j'=5$.

In order to gain insight into the mechanism of electric field control of reaction cross sections and product state distributions, we focus on the the dominant reactive transition $j=0 \rightarrow j'=5$. In Fig. 3, we plot the contributions of the different partial wave transitions $j=0, \ell=0 \rightarrow j', \ell'$ as a function of the electric field strength. Since the total angular momentum of the collision complex $\mathbf{J} = \mathbf{j} + \mathbf{\ell} = \mathbf{j}' + \mathbf{\ell}'$ is conserved at zero field, and $j=\ell=0$ in the entrance reaction channel (assuming *s*-wave scattering), it follows that $j'+\ell'=0$ and hence $\ell'=j'$. Thus only the $\ell'=5$ partial wave contribution is allowed at zero field. The line with circles in Fig. 3 confirms this. An external field induces couplings between the adjacent J states [17, 19]. As a result, the off-diagonal, J -changing transitions $j=0, \ell=0 \rightarrow j', \ell'=j' \pm 1$ become allowed, as illustrated in Fig. 3. While these J -changing transitions play a minor role at low fields, they become dominant at fields above 100 kV/cm. As shown in the inset of Fig. 3, the J -changing transitions $\ell=0 \rightarrow \ell'=6, 7$ make up more than 70% of the reaction cross section at $E = 125$ kV/cm (on resonance B). We therefore refer to resonance B as

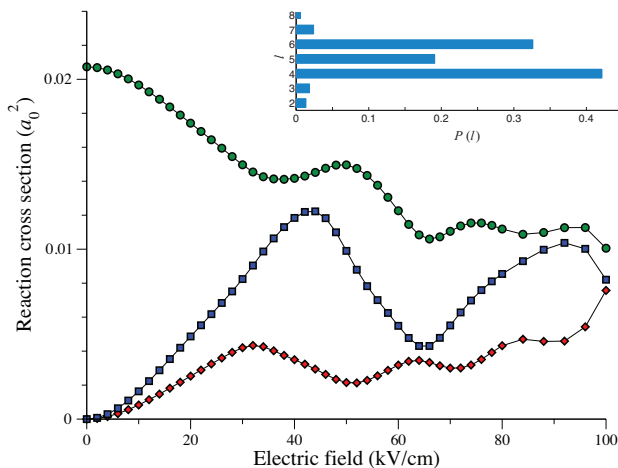


Fig. 3: Partial wave contributions to the cross section for the $\text{LiF}(v=1, j=0) \rightarrow \text{HF}(v'=0, j'=5)$ reactive transition as functions of an applied electric field. This transition dominates the total reaction cross section in the range of electric fields close to the resonance triplet (see Fig. 2). Circles – J -conserving transition $\ell=0 \rightarrow \ell'=5$, squares and diamonds – J -changing transitions $\ell=0 \rightarrow \ell'=4, 6$. The inset shows the individual partial wave contribution to the $j=0 \rightarrow j'=5$ reactive cross section on resonance at $E=125$ kV/cm. The collision energy $E_C=0.01$ cm $^{-1}$.

the *electric-field-induced* resonance.

Further analysis shows that the elastic cross section does not vary significantly as the electric field is tuned across the resonance region ($E=124.5-127$ kV/cm). This strongly suggests that the resonant enhancement of the reaction cross section shown in Fig. 2 is due to a resonance in the *outgoing* reaction channel [29]. This type of resonance is mediated by anisotropic coupling between the $\ell=0$ incoming state and an $\ell'=2$ state trapped behind the centrifugal barrier in the product channel [29]. The anomalously cold rotational state distribution at $E=124$ kV/cm reflects the decay mechanism of the reactive scattering resonance.

While the electric-field-induced resonances can greatly enhance the reaction cross section, the excess vibrational energy of the $\text{LiF}(v=1, j=0)$ reactants can also be converted into translational energy via non-reactive collisions leading to vibrational relaxation. To explore the possibility of controlling the relative efficiency of these competing pathways, we plot in Fig. 4 the electric field dependence of the ratio of cross sections for vibrational relaxation and reactive scattering. At low fields, the branching ratio varies insignificantly, and vibrational relaxation remains as efficient as it is at zero field. Near the electric field-induced resonance, however, the branching ratio drops to 4 before raising back to 10.

The electric field dependence of the $\text{LiF}(v=0, j')$ product distribution following vibrational relaxation in $\text{LiF}(v=1, j=0) + \text{H}$ collisions is plotted in the inset of Fig. 4 as a function of j' . We observe strong variation of the distributions even at low electric fields.

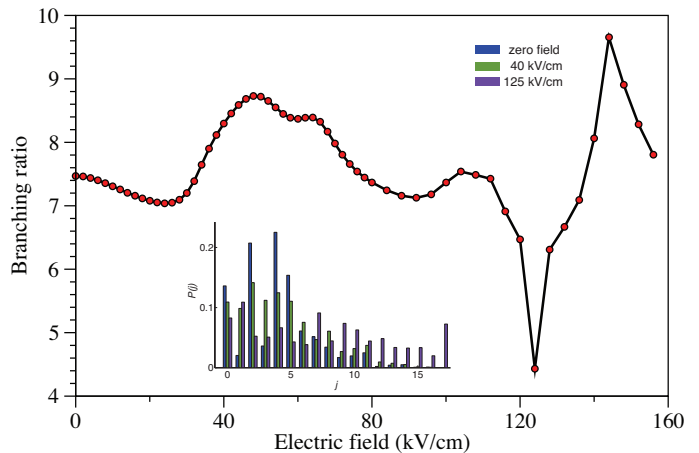


Fig. 4: The branching ratio for inelastic to reactive cross sections as a function of electric field. The inset shows rotational product state distributions for vibrational relaxation in non-reactive $\text{LiF}(v=1, j=0) + \text{H}$ collisions.

A moderate field of 40 kV/cm broadens the distribution significantly, populating higher j' -states. We attribute this effect to the field-induced hybridization of LiF rotational states in the $v=0$ manifold, which modifies the anisotropic part of the LiF-H interaction potential and changes the relative populations of final rotational states. At the resonance B, the rotational distribution becomes extremely broad and multimodal. We note that while near-resonant rovibrational energy transfer in $\text{LiF}(v=1, j=0) + \text{H}$ collisions is forbidden at low-to-moderate electric fields, it becomes allowed at $E=125$ kV/cm, signalling a profound change in the mechanism of rovibrational energy transfer near electric field-induced scattering resonances [35].

In conclusion, we have introduced an efficient theoretical method for solving the quantum reactive scattering problem in the presence of an external field based on a hyperspherical coordinate formalism [14–16] combined with the total angular momentum representation for molecular collisions in external fields [18, 19]. The method makes it possible to obtain for the first time numerically converged results for a three-dimensional atom-diatom chemical reaction in a DC electric field. Our methodology can be applied to any atom-diatom chemical reaction in a magnetic, DC electric and off-resonant microwave and laser fields. As a first application, we focus on the prototype chemical reaction $\text{LiF}(v=1, j=0) + \text{H} \rightarrow \text{Li} + \text{HF}$. Our calculations show that the strength of DC electric fields achievable in the laboratory is sufficient to induce scattering resonances that modify dramatically the total reaction probabilities, the branching ratios for reactive vs inelastic scattering and the rotational distributions of the reaction products. They also show that electric fields modify dramatically the rotational distributions of the products of vibrationally inelastic scattering.

The accuracy of *ab initio* calculations of atomic [36] and molecular [37] PESs is improving rapidly, with recent state-of-the-art calculations approaching a level of precision of $<0.5 \text{ cm}^{-1}$ sufficient for robust prediction of atom-atom scattering properties at ultralow temperatures [36]. Until such a PES is developed for Li-HF, quantum scattering simulations should be used in tandem with experimental measurements of reaction rates to refine the existing PES, as done for non-reactive

collisions in the presence of external fields [31, 36]. The methodology developed in this work enables accurate coupled-channel calculations on chemical reactions in external fields, thereby making possible this crucial synergy between theory and experiment.

This work was supported by NSERC of Canada. We are grateful to D. Ding for his expert assistance with high-performance computing.

-
- [1] R. N. Zare, *Science* **279**, 1875 (1998).
 - [2] M. Shapiro and P. Brumer, *Principles of the Quantum Control of Molecular Processes* (New Jersey: Wiley Inter-Science, 2003).
 - [3] S. A. Rice and M. Zhao, *Optical Control of Molecular Dynamics* (Wiley, New York, 2000).
 - [4] R. V. Krems, *Phys. Chem. Chem. Phys.* **10**, 4079 (2008).
 - [5] D. Herschbach, *Faraday Discuss.* **142**, 9 (2009).
 - [6] L. D. Carr, D. DeMille, R. V. Krems, and J. Ye, *New J. Phys.* **11**, 055049 (2009).
 - [7] K.-K. Ni, S. Ospelkaus, D. Wang, G. Quémener, B. Neyenhuis, M. H. G. de Miranda, J. L. Bohn, J. Ye, and D. S. Jin, *Nature* **464**, 1324 (2010).
 - [8] M. H. G. de Miranda, A. Chotia, B. Neyenhuis, D. Wang, G. Quémener, S. Ospelkaus, J. L. Bohn, J. Ye, and D. S. Jin, *Nat. Phys.* **7**, 502 (2011).
 - [9] G. Quémener and P. S. Julienne, *Chem. Rev.* **112**, 4949 (2012).
 - [10] B. K. Stuhl, M. T. Hummon, and J. Ye, *Annu. Rev. Phys. Chem.* **65**, 501 (2014).
 - [11] G. Quémener and J. L. Bohn, *Phys. Rev. A* **81**, 022702 (2010).
 - [12] Z. Idziaszek, and P. S. Julienne, *Phys. Rev. Lett.* **104**, 113202 (2010).
 - [13] B. Gao, *Phys. Rev. Lett.* **105**, 263203 (2010).
 - [14] R. T. Pack and G. A. Parker, *J. Chem. Phys.* **87**, 3888 (1987).
 - [15] D. Skouteris, J. F. Castillo, and D. E. Manolopoulos, *Comp. Phys. Commun.* **133**, 128 (2000).
 - [16] G. C. Schatz, *Chem. Phys. Lett.* **150**, 92-98 (1988).
 - [17] T. V. Tscherbul, and R. V. Krems, *J. Chem. Phys.* **129**, 034112 (2008).
 - [18] T. V. Tscherbul and A. Dalgarno, *J. Chem. Phys.* **133**, 184104 (2010).
 - [19] T. V. Tscherbul, *Phys. Rev. A* **85**, 052710 (2012).
 - [20] See the Supplementary Material for the expressions for the matrix elements of the molecule-field interaction Hamiltonian, reactive scattering boundary conditions in the presence of electric fields, and convergence tests.
 - [21] S. C. Althorpe and D. Clary, *Annu. Rev. Phys. Chem.* **54**, 493 (2003).
 - [22] A. Aguado, M. Paniagua, C. Sanz, and O. Roncero, *J. Chem. Phys.* **119**, 10088 (2003).
 - [23] P. F. Weck and N. Balakrishnan, *J. Chem. Phys.* **122**, 234310 (2005).
 - [24] R. Bobbenkamp, H. Loesch, M. Mudrich, and F. Stienkemeier, *J. Chem. Phys.* **135**, 204306 (2011).
 - [25] H. F. Hess, G. P. Kochanski, J. M. Doyle, N. Masuhara, D. Kleppner, and T. J. Greytak, *Phys. Rev. Lett.* **59**, 672 (1987).
 - [26] A. W. Wiederkehr, S. D. Hogan, B. Lambillotte, M. Andrist, H. Schmutz, J. Agner, Y. Salathé, and F. Merkt, *Phys. Rev. A* **81**, 021402(R) (2010).
 - [27] J. E. van den Berg, S. C. Mathavan, C. Meinema, J. Nauta, T. H. Nijbroek, K. Jungmann, H. L. Bethlem, and S. Hoekstra, *arXiv:1402.2800v1* (2014).
 - [28] N. R. Hutzler, H.-I. Lu, and J. M. Doyle, *Chem. Rev.* **112**, 4803 (2012).
 - [29] B. Zygelman and A. Dalgarno, *J. Phys. B* **35**, L441 (2002).
 - [30] E. Tiesinga, B. J. Verhaar, and H. T. C. Stoof, *Phys. Rev. A* **47**, 4114 (1993).
 - [31] W. C. Campbell, T. V. Tscherbul, H.-I. Lu, E. Tsikata, R. V. Krems, and J. M. Doyle, *Phys. Rev. Lett.* **102**, 013003 (2009).
 - [32] J. L. Bohn, M. Cavagnero, and C. Ticknor, *New J. Phys.* **11**, 055039 (2009).
 - [33] M. Qiu *et al.*, *Science* **311**, 1440 (2006).
 - [34] W. Dong, C. Xiao, T. Wang, D. Dai, X. Yang, and D. H. Zhang, *Science* **327**, 1501 (2010).
 - [35] R. C. Forrey, N. Balakrishnan, A. Dalgarno, M. R. Haggerty, and E. J. Heller, *Phys. Rev. Lett.* **82**, 2657 (1999).
 - [36] S. Knope, P. S. Żuchowski, D. Kedziera, L. Mentel, M. Puchalski, H. P. Mishra, A. S. Flores, and W. Vassen, *arXiv:1404.4826v1* (2014).
 - [37] W. Skomorowski, F. Pawłowski, T. Korona, R. Moszynski, P. S. Żuchowski, and J. M. Hutson, *J. Chem. Phys.* **134**, 114109 (2011).